

1 **When the species is also a habitat: comparing the predictively modelled distributions**
2 **of *Lophelia pertusa* and the reef habitat it forms.**

3 **Kerry L. Howell^a, Rebecca Holt^a, Inés Pulido Endrino^a, Heather Stewart^b**

4 a. Marine Biology and Ecology Research Centre, Marine Institute at the University of Plymouth, Drake
5 Circus, Plymouth, PL3 5EE. UK. Email: kerry.howell@plymouth.ac.uk

6 b. British Geological Survey, Murchison House, West Mains Road, Edinburgh, EH9 3LA. UK. Email:
7 hast@bgs.ac.uk

8

9 Corresponding authors details: Email: kerry.howell@plymouth.ac.uk Tel: +44 (0)1752 584544

10

11 **Abstract**

12 Internationally there is political momentum to establish networks of marine protected
13 areas for the conservation of threatened species and habitats. Practical
14 implementation of such networks requires an understanding of the distribution of
15 these species and habitats. Predictive modelling provides a method by which
16 continuous distribution maps can be produced from limited sample data. This method
17 is particularly useful in the deep sea where a number of biological communities have
18 been identified as vulnerable ‘habitats’, including *Lophelia pertusa* reefs. Recent
19 modelling efforts have focused on predicting the distribution of this species. However
20 the species is widely distributed where as reef habitat is not. This study uses Maxent
21 predictive modelling to investigate whether the distribution of the species acts as a

22 suitable proxy for the reef habitat. Models of both species and habitat distribution
23 across Hatton Bank and George Bligh Bank are constructed using multibeam
24 bathymetry, interpreted substrate and geomorphology layers, and derived layers of
25 bathymetric position index (BPI), rugosity, slope and aspect. Species and reef presence
26 records were obtained from video observations. For both models performance is fair
27 to excellent assessed using AUC and additional threshold dependant metrics. 7.17% of
28 the study area is predicted as highly suitable for the species presence while only 0.56%
29 is suitable for reef presence, using the sensitivity-specificity sum maximization
30 approach to determine the appropriate threshold. Substrate is the most important
31 variable in the both models followed by geomorphology in the RD model and fine scale
32 BPI in the SD model. The difference in the distributions of reef and species suggest that
33 mapping efforts should focus on the habitat rather than the species at fine (100m)
34 scales.

35

36 Keywords: deep-sea; *Lophelia pertusa*; habitat mapping; biotopes; marine protected
37 area; maxent;

38

39 **1. Introduction**

40 The call for better spatial management of our marine environment is growing globally.
41 Specifically, there is momentum for the establishment of networks of marine
42 protected areas (MPAs) driven by global, European and (within the UK) national

43 initiatives. One of the criteria by which MPAs are selected includes the protection of
44 habitats and species that have been identified as rare, sensitive, functionally
45 important, threatened and / or declining.

46

47 Within the NE Atlantic region the 1992 Convention for the Protection of the Marine
48 Environment of the north-east Atlantic (OSPAR Convention) gives the OSPAR
49 Commission a duty to develop means, consistent with international law, for
50 establishing protective, conservation, restorative or precautionary measures related to
51 specific species or habitats. A target date of 2010 has been set by OSPAR contracting
52 parties to achieve “an ecologically coherent network of well managed Marine
53 Protected Areas” that serve (at least in part) to protect those habitats and species
54 listed under Annex V of the Convention, on the OSPAR List of Threatened and/or
55 Declining Species and Habitats.

56

57 At a European level the EU Habitats and Species Directive (92/43/EEC) requires the
58 establishment of protected areas (Special Areas of Conservation – SACs) for habitats
59 and species listed under Annex I and V respectively of the Directive, in areas of sea
60 under the jurisdiction of member states (i.e. out to the 200 nm limit). In addition, the
61 2006 United Nations General Assembly Resolution 61/105 called “upon States to take
62 action immediately, individually and through regional fisheries management
63 organizations and arrangements, and consistent with the precautionary approach and
64 ecosystem approaches, to sustainably manage fish stocks and protect vulnerable

65 marine ecosystems [VMEs], including seamounts, hydrothermal vents and cold water
66 corals, from destructive fishing practices". This resolution has also ultimately resulted
67 in the establishment of MPAs for the protection of specific species and habitats.

68

69 In order to establish MPAs for the protection of listed habitats and species there is a
70 clear need to have a firm understanding of the distribution of those species and
71 habitats (i.e. maps). The difficulties and expense of collecting species and habitat
72 distribution data has led to the approach of using surrogates (Howell, 2010) and / or
73 predictive species modelling techniques to provide maps of the distribution of
74 vulnerable species (Bryan & Metaxas 2007; Holmes et al., 2007; Embling et al., 2010).
75 This approach is particularly useful for the deep-sea and high seas. Here, the vast area
76 involved, sparse and highly localised data available, and distance from land, compound
77 the problems encountered in shallow water settings. Within the deep-sea (high seas)
78 ecosystem there are few actual species that are listed as of conservation concern
79 under the legislation detailed above. Only commercially important fish species
80 including orange roughy (*Hoplostethus atlanticus*), Portuguese dogfish (*Centroscymnus*
81 *coelolepis*), and Leafscale gulper shark (*Centrophorus squamosus*), known to have
82 undergone significant declines (ICES, 2008; ICES, 2010) are included. However a
83 number of deep-sea habitats are listed. These habitats are predominantly biogenic in
84 origin or are in fact biological assemblages, and include *Lophelia pertusa* reefs, coral
85 gardens, sponge aggregations and sea-pen and burrowing megafauna communities, as

86 well as other geogenic habitats such as carbonate mounds, seamounts, and oceanic
87 ridges with hydrothermal vents/fields.

88

89 Recently, efforts have been made to model the distribution of the cold water coral *L.*
90 *pertusa* from global to local scales, in order to identify areas of conservation
91 importance (Davies et al., 2008; Dolan et al., 2008; Guinan et al., 2009; Tittensor et al.,
92 2009). *L. pertusa* is a widely distributed species and occurs as isolated colonies on
93 boulders, cobbles, sand ripples, and even flat sea bed where some form of hard
94 substrate is available for attachment (Wilson, 1979; Mortensen and Buhl-Mortensen,
95 2004a, b; Hovland et al., 2005). Its conservation importance stems from its reef
96 forming capacity. *L. pertusa* can form large reefs and giant carbonate mounds up to
97 300m high and several km in diameter (Roberts et al., 2006). Reef structures are highly
98 biodiverse, possibly rivalling tropical coral reefs (Roberts et al., 2006). They may also
99 have an important role as essential fish habitat but this is not yet clear (Husebø et al.,
100 2002; Auster, 2005; Costello et al., 2005). *L. pertusa* only forms reefs under specific
101 environmental conditions that are not yet fully understood but are controlled by the
102 interplay between local hydrography and sedimentary dynamics (Thiem et al., 2006).

103

104 Given that the species is widely spread while the reef habitat has specific
105 environmental requirements likely to result in a more confined distribution, to what
106 extent does the distribution of *L. pertusa* species act as a proxy for the reef habitat?
107 Mapping efforts that focus on the species rather than the habitat may produce maps

108 of limited use to marine environmental managers if the distribution of the species is so
109 broad as to indicate reef habitat is widely spread. Using the species distribution as a
110 proxy for the habitat could provide a false impression of the extent of reef habitat and
111 effect assessments of rarity and threat from human activities. The aim of this study is
112 to use predictive modelling to investigate the difference in the distribution of the
113 species and habitat and assess the implications of any difference to marine
114 environmental management. Multibeam bathymetry, interpreted substrate and
115 geomorphology layers, and derived layers of bathymetric position index (BPI), rugosity,
116 slope and aspect are used as environmental input layers together with presence of *L.*
117 *pertusa* reef and species. Here we conform to the definition of *L. pertusa* reef following
118 Roberts et al (2006) as biogenic structures formed by *L. pertusa* frameworks that alter
119 sediment deposition, provide complex structural habitat and are subject to the
120 processes of growth and (bio)erosion. However, presence data are derived from
121 records of living *L. pertusa* reef only and not dead framework structures. The study
122 focuses on Hatton and George Bligh Banks in the N.E. Atlantic.

123

124 **2. Methods**

125 **2.1 Site description**

126 Hatton Bank and George Bligh Bank are part of the Rockall Plateau (Hitchen, 2004),
127 which is a large piece of continental crust that separated from the European continent
128 during the early Cretaceous (Hauterivian-Cenomanian) when the North Atlantic was in
129 the early stages of formation (Musgrove and Mitchener, 1996) (Fig. 1). Hatton Bank

130 forms an elongate arc that stretches over 400 km and descends >2500 m below sea
131 level into the Iceland Basin to the west and 1100 m below sea level into the Hatton
132 Basin, (sometimes referred to as the Hatton-Rockall Basin), to the east. At its summit
133 Hatton Bank lies less than 500 m below sea level. South of 59°N Hatton Bank is
134 orientated approximately southwest-northeast, further north the orientation is more
135 east-west. George Bligh Bank is broadly conical in shape and situated at the north-
136 eastern end of the Rockall Plateau (and Hatton Basin). It rises to a summit at 450 m
137 below sea level, and has a diameter of roughly 75 km.

138

139 **2.2 Data collection**

140 Collection of biological (video) data and low resolution multibeam data from both
141 Hatton Bank and George Bligh Bank were undertaken over a one month period
142 (August-September) in 2005 using the commercial research vessel *S/V Kommandor*
143 *Jack*. Further collection of biological data and collection of higher resolution multibeam
144 data were undertaken over a two month period (August – October) in 2006 using the
145 commercial research vessel *M/V Franklin*. Video sampling stations were selected
146 during operations using multibeam bathymetry and backscatter data. Video tows were
147 selected to cover a range of geomorphology, substrate types and water depths (Fig. 1).

148

149 Video data were collected using the Seatronics drop frame camera system. The system
150 comprised an integrated DTS 6000 digital video telemetry system, which provided a

151 real time video link to the surface, and a digital stills camera (5 mega pixel, Kongsberg
152 OE14-208). In the 2005 surveys, the video stream from the viewing screen of the
153 digital stills camera provided video data, in 2006 separate video (Kongsberg 14-366)
154 and stills cameras were used. Cameras were mounted at an oblique angle (video: 24°;
155 stills: 22° from the horizontal) to the sea bed to aid in species and habitat
156 identification. Sensors monitored depth and altitude, and an Ultra Short Base Line
157 (USBL) beacon provided accurate (to approximately 1m) position data for the camera
158 frame.

159

160 The system was deployed from the starboard side of the vessel. Video tows were
161 between 250 and 1200 m long. For the majority of tows, vessel speed was
162 approximately 0.5 knots (min 0.3 and max 0.7 knots), with most tows lasting between
163 0.5 and 1.5 h. The drop frame was towed in the water column between one and three
164 metres (dependant on substrate type, topography and currents) above the sea bed. At
165 the beginning of each tow, starting from when the sea floor became visible, a 2-3
166 minute period was allowed before sampling, to enable the camera to stabilise before
167 commencing the transect.

168

169 Videos were reviewed and the occurrence of *L. pertusa* colonies and *L. pertusa* reef
170 habitat noted and linked to the navigational data from the USBL on the camera system,
171 such that the location of each colony / habitat occurrence was recorded. Presence
172 data for both species and habitat were then plotted in ArcGIS 9.3.

173

174 **2.3 Multibeam**

175 Multibeam data were acquired in 2005 on *S/V Kommander Jack* using an EM120 (12
176 kHz; 191 beams) multibeam echosounder system which achieved good quality
177 bathymetric data with marginal quality backscatter data. During the 2005 survey
178 complete data coverage was achieved through 2500m line spacing on Hatton Bank and
179 1500m line spacing on the other survey areas. In 2006 multibeam data were acquired
180 on *M/V Franklin* using an EM1002 (95 kHz; 111 beams) multibeam echosounder
181 system which achieved excellent quality bathymetric and moderate quality backscatter
182 data. During the 2006 survey complete data coverage was achieved through 650m line
183 spacing on Hatton Bank and 500m line spacing on the other survey areas. It should be
184 noted that weather and sea conditions adversely impacted on the backscatter data
185 quality during both the 2005 and 2006 surveys. Positioning was accomplished using
186 real-time Differential GPS (DGPS) systems. The C-Nav system was used in 2005 and the
187 ARON 2000 system in 2006. All data acquisition systems took their time stamp from
188 the primary DGPS which had a theoretical accuracy of better than 0.5m. Sound velocity
189 measurements were performed at regular intervals to account for hydrology effects
190 during both surveys. Multibeam data were processed onboard ship and ashore by
191 OSAE Ltd in 2005 and Marin Mätteknik AB in 2006. Data were gridded at resolutions
192 appropriate to the quality of the data (2005: 200m grids; 2006: 25m grids). Minimum
193 waters depths encountered over Hatton Bank were -483m, Lyonesse Seamount -507m
194 and George Bligh Bank -435m. The maximum water depth of -1679m was encountered

195 on the eastern flank of George Bligh Bank as it descends into the Rockall Trough. As
196 Maxent requires all environmental data to have the same geographic bounds and cell
197 size the 2006 multibeam dataset was regrided in ArcGIS 9.3 to a 200m grid and
198 merged with the 2005 multibeam dataset to produce a single bathymetry data layer,
199 which was used to produce subsequent derived layers (see section 2.4).

200

201 **2.4 Derived layers**

202 Additional environmental layers included in the model were layers derived from the
203 multibeam bathymetry and were generated in ArcGIS using the spatial analyst and
204 benthic terrain modeller extensions. Derived layers included slope, rugosity (indicates
205 the ratio of surface area to planar area), aspect (identifies the direction of the steepest
206 slope) and bathymetric position index at broad and fine scale.

207

208 Bathymetric Position Index (BPI) is a measure of where a referenced location is relative
209 to the locations surrounding it. Derived from an input bathymetric data set, a
210 neighbourhood analysis function produces an output raster in which the output cell
211 value at each location is a function of the input cell value and the values of the cells in
212 a specified "neighborhood" surrounding that location. As bathymetric position is an
213 inherently scale-dependent phenomenon (Weiss, 2001) both fine scale and broad scale
214 BPI data sets are usually created, whereby the fine scale BPI layer is generated using a
215 smaller analysis neighbourhood than the broad scale BPI layer. In the present study

216 the default settings used in the Benthic Terrain Modeller extension to ArcGIS were
217 applied to calculate coarse scale and fine scale BPI layers. These are, for broad scale
218 BPI: inner radius = 1, outer radius = 5, and fine scale: inner radius = 1, outer radius = 3.
219 Positive cell values within a BPI data set denote features and regions that are higher
220 than the surrounding area. Conversely negative cell values within a BPI data set denote
221 features and regions that are lower than the surrounding area. BPI values near zero
222 are either flat areas (where the slope is near zero) or areas of constant slope (where
223 the slope of the point is significantly greater than zero) (Weiss, 2001).

224

225 **2.5 Sea-bed Substrate and Geomorphological Interpretations**

226 All data were used to produce ArcGIS layers of sea-bed substrate and
227 geomorphological features. For each digital stills image acquired a sea-bed sediment
228 classification was assigned. These point classifications were used to ground-truth the
229 multibeam echosounder and backscatter data allowing a complete sea-bed substrate
230 interpretation to be created utilising all available data layers including derived layers. It
231 should be noted that the backscatter quality was not suitable for accurate habitat
232 differentiation as poor weather conditions and sea-state introduced noise which
233 masked the more subtle geological variations of the sea floor. Following the sea-bed
234 substrate classification, a geomorphological interpretation was created using standard
235 geological terms and definitions. Geomorphology from the study area is described by
236 10 classes, with substrate described by 9 classes (Table 1).

237

238 The following 8 environmental data layers were prepared in ArcGIS 9.3 for use in
239 Maxent: continuous variables - bathymetry, slope, aspect, fine scale BPI, broad scale
240 BPI, rugosity, categorical variables - substrate and geomorphology.

241

242 **2.6 Maximum Entropy Modelling**

243 Maximum entropy modelling was introduced as a general approach to presence only
244 modelling of species distributions by Phillips et al. (2004; 2006). It has subsequently
245 been shown to perform very well against other presence only models (Elith et al.,
246 2006) with specific comparisons made between Maxent and environmental niche
247 factor analysis (ENFA) applied to predictions of the global distribution of stony corals
248 (Tittensor et al., 2009). Maxent estimates a target probability distribution by finding
249 the probability distribution of maximum entropy subject to a set of constraints that
250 represent our incomplete information about the target distribution (Phillips et al.,
251 2006). Put simply and in the context of the present study Maxent allows the user to
252 predict the distribution of a species/ habitat in terms of probability of occurrence, by
253 finding the distribution that agrees with everything known about the distribution of
254 the species / habitat (given the environmental data that has been provided to the
255 model), without making any assumptions about what is not known.

256

257 Single models were constructed for *L. pertusa* species distribution (SD) and *L. pertusa*
258 reef distribution (RD) using Maxent version 3.3.2, available for free download on

259 <http://www.cs.princeton.edu/~schapire/maxent/>. Maxent was run with default
260 settings: convergence threshold 10^{-5} and maximum number of iterations of 500,
261 regularisation set to 1, that have been shown to achieve good performance (Phillips
262 and Dudík, 2008) even with small size datasets. However, for the RD model following
263 visual inspection of the response curves and subsequent trials with increased
264 regularisation, the regularisation parameter was set to 2 to reduce over fitting of the
265 model. Maxent results are given in a logistic system where values near 0 mean low
266 probability of presence and values near 1 mean high probability of presence.

267

268 **2.7 Model evaluation**

269 The models generated were evaluated in two ways.

270

271 Firstly, threshold independent ROC (receiver operating characteristic) curves were
272 used to measure how successful the prediction was using the area under the curve
273 (AUC) (Fielding & Bell, 1997). As a result of the sampling method used (video
274 transects), the presence data for both SD and more obviously for RD were spatially
275 autocorrelated within transects. To attempt to account for this in the model evaluation
276 process cross validation of the both models was performed manually rather than using
277 the Maxent replicates setting. For the SD model 1479 presence records (reduced to
278 102 cells with presence records) were obtained from 43 transects. These data were
279 partitioned such that approximately 25% of the transects (10 or 11) constituting ~25-
280 30% of the presence records were omitted from model building and used as a test
281 dataset. This process was repeated 10 times and average AUC and standard deviation

282 of AUC across all 10 models was calculated. For the RD model the nature of the reef
283 presence data was such that although there were 9 cells with reef presence, in truth
284 this amounted to observation of 6 complete reefs (as one reef occupied more than one
285 cell). Therefore cross validation of the RD model was performed by splitting the
286 presence data into groups corresponding to the 6 reefs observed and using these data
287 to manually run the Maxent model 6 times, leaving out one 'complete reef' presence
288 each time. Average AUC and standard deviation of AUC across all 6 models was
289 calculated. However the small total number of presence samples available to the
290 model suggests that cross validation may be inappropriate given that test data sets
291 may consist of a single presence point.

292

293

294 Secondly, the model assessment indices: percent correctly classified (PCC), specificity
295 and sensitivity (Fielding & Bell, 1997), were calculated using the Presence-Absence
296 Model Evaluation library (Freeman, 2007) in R (R Development Core Team, 2010).
297 These indices require that a threshold be used to convert the continuous Maxent
298 probability of occurrence prediction to a binary prediction delimiting presence or
299 absence. Determining the appropriate threshold for Maxent models is an interesting
300 and ongoing area of research (Liu et al., 2005). In this study three possible thresholds
301 were assessed for their use in producing a reliable binary output map (Table 2). The
302 three selected for testing were from the group of metrics identified as 'good' by Liu et
303 al. (2005). The effectiveness of each threshold was evaluated in R (R Development Core
304 Team, 2010) using the Presence-Absence Model Evaluation library (Freeman, 2007)

305 and model assessment indices listed previously. For SD and RD models the model build
306 datasets were used together with absence data obtained from video analysis to assess
307 the appropriateness of the thresholds. In addition thresholds were also assessed for
308 each of the training and test model datasets and average performance of each
309 threshold calculated. The most appropriate threshold was defined as that which
310 resulted in constantly delivering the highest sensitivity score, since the precautionary
311 principle suggests that false positives are less of a concern than false absences. For this
312 study the sensitivity-specificity sum maximization approach where the sum of
313 sensitivity and specificity is maximized Cantor et al. (1999), was selected (Table 2).

314

315 **2.8 Assessment of variable importance within the models**

316 Jackknife tests were undertaken to assess variable importance during model
317 development by comparing the model gain (a measure of goodness of fit closely
318 related to deviance) associated with models constructed with each variable omitted in
319 turn, models constructed using individual variables only, and the full final model.
320 Relative changes in gain between the full model and models constructed without one
321 variable and with only one variable allow an assessment of relative importance of each
322 variable to the final model build.

323

324 **2.9 Quantification of species and habitat distribution**

325 Binary maps for both SD and RD predicted distribution, produced using the sensitivity-
326 specificity sum maximization approach threshold obtained for the full models (SD=0.2,
327 RD=0.25), were used to quantify the difference in area suitable for *L. pertusa* species
328 and *L. pertusa* reef habitat in ArcGIS 9.3.

329

330 **3. Results**

331 **3.1 Model evaluation**

332 For all partitions of the occurrence data, for both the *Lophelia pertusa* species
333 distribution (SD) and *Lophelia pertusa* reef distribution (RD) models, the AUC values
334 achieved by the training-test data were better than random (Table 3) (AUC>0.5). Full
335 model AUC and mean training and test AUC for both SD and RD models could be rated
336 a fair (0.7-0.8), good (0.8-0.9) or excellent (0.9-1). However, the consistently higher
337 AUC value for the RD training-test models and the higher AUCs for the full model
338 (Table 3) indicates that the whole RD model can better discriminate between suitable
339 and unsuitable distribution areas for *L. pertusa* reef than for *L. pertusa* species.

340

341 Threshold dependent model assessment indices for the sensitivity-specificity sum
342 maximization approach threshold also indicated that, when measured using PCC and
343 sensitivity, the SD models performance was generally fair, while the RD models
344 performance was generally excellent. Specificity scores for the SD models ranged

345 between awful (<0.6), poor (0.6-0.7) and good (0.8-0.9) reflecting the decision to select
346 a threshold to maximise sensitivity scores.

347

348 **3.2 Importance of environmental variables within each model**

349 Jackknife tests of variable importance revealed the models generated for both SD and
350 RD relied heavily on the substrate variable both in terms of having the most useful
351 information by itself and having the most information that was not present in the
352 other variables (Fig. 2). Analysis of response curves created through construction of
353 Maxent models using single variables illustrated the dependence of predicted
354 suitability on substrate, with the bedrock, gravel and sandy gravel categories as most
355 important in the SD model and bedrock as most important in the RD model (Fig. 3).

356

357 Within the RD model geomorphology was the second most important variable in terms
358 of having the most useful information by itself, but was of limited importance to the
359 SD model (Fig. 2). The geomorphological categories flank, pinnacle/mound, ridge, and
360 escarpment were of most use. However, for both SD and RD models omission of the
361 geomorphological variable resulted in the second largest drop in gain after depth and
362 substrate respectively suggesting that the geomorphological layer contained
363 information that was not present in the other variables (Fig. 2).

364

365 For both SD and RD models fine scale BPI and broad scale BPI were the next most
366 important variables in terms of providing the highest gain when used in isolation to
367 construct models (Fig. 2). As the information in one BPI layer was essentially also
368 contained in the other BPI layer, albeit at different resolution, in order to fully assess
369 the importance of BPI to the SD and RD models, both models were rerun including only
370 one BPI variable. However, in both the original models and the rerun models there was
371 a negligible change in gain when BPI was omitted in jackknife analyses. This suggests
372 that BPI does not contain any information that was not present in other variables.
373 Analysis of response curves illustrated subtle differences between models in the
374 dependence of predicted suitability on both fine scale and broad scale BPI. Within the
375 SD model both high negative values and high positive values were of greatest
376 importance (Fig. 3). However within the RD model only high positive values were of
377 greatest importance.

378

379 Within the SD model rugosity and slope were the next most important variables (Fig.
380 2). However, omission of the slope or rugosity variable in jackknife tests resulted in a
381 negligible drop in training gain. This suggests neither variable contained information
382 that was not present in other variables. Analysis of response curves suggested the
383 highest probability of occurrence of SD was achieved at rugosity of >1.01 and slopes of
384 >20° (Fig. 3).

385

386 Jackknife tests of variable importance suggested that for both models bathymetry was
387 of limited importance alone, however omission of the bathymetry variable from the
388 models resulted in the third largest drop in training gain, suggesting the bathymetry
389 variable contained information not present in other variables (Fig. 2). Heuristic
390 estimates of relative contributions of the environmental variables to the Maxent
391 model suggests that for SD and RD models bathymetry contributed 14.7% and 0.7%
392 respectively. Analysis of response curves suggest the depths that resulted in the
393 highest probability of SD presence were 500-900m, however for RD the probability of
394 presence was predicted to increase with depth (Fig. 3), most likely a reflection of the
395 limited depth range sampled.

396

397 Aspect was of least importance in both SD and RD models (Fig. 2) although
398 interestingly probability of species occurrence was lowest at a bearing of 300°.

399

400 **3.3 Potential distribution of *Lophelia pertusa* species and reef**

401 Binary maps (1-presence, 0-absence) of both species and habitat distribution show *L.*
402 *pertusa* species is distributed over a broader area (7.17% of the map area) than *L.*
403 *pertusa* reef habitat (0.56% of the map area) (Fig. 4).

404

405 **4. Discussion**

406 **4.1 Species vs habitat distribution**

407 On Hatton Bank and George Bligh Bank, the models identify a broader area of high
408 suitability for the species than for reef (7.17% vs 0.56% of the total area respectively
409 using the sensitivity-specificity sum maximization threshold). Visual analysis of the
410 spatial distribution of areas predicted as highly suitable for species and reef suggests
411 that reef distribution is a highly restricted subset of species distribution.

412

413 Within the SD model the species was associated with bedrock, gravel and sandy gravel
414 substrate categories, with no one geomorphological class of particular importance.
415 These findings support what is currently known of the ecology of this species. *L.*
416 *pertusa* has a cosmopolitan distribution (Zibrowius, 1980) and occurs as individual
417 colonies under a relatively broad range of conditions, from depths of 40-3400m,
418 temperatures of between 4-13°C, salinities of 32-38‰ and across different oceans
419 including the NE Atlantic, Barents Sea, the Mediterranean, and the Gulf of Mexico
420 (Freiwald et al, 2004). *L. pertusa* is found on hard and mixed bottoms (Dons 1944;
421 Frederiksen et al., 1992) and in areas of fine sand where some form of hard substrate
422 is present for initial attachment. Wilson (1979) suggested that suitable substrata for
423 colony growth may be small e.g. mollusc shells, cobbles and boulders. It is not
424 surprising then, to find that the species is likely to be found over a relatively wide area

425

426 In comparison to the species, *L. pertusa* reef habitat is not widely distributed. The RD
427 model indicates that reef habitat is only likely to be present over small areas on both
428 Hatton Bank and George Bligh Bank. Within the wider NE Atlantic a limited number of

429 large reef structures (mound regions) have been identified (see Wheeler et al, 2007 for
430 a review). *L. pertusa* only forms reefs under a specific set of environmental conditions.
431 The largest reefs occur in depths between 500-1200m (Frederiksen et al., 1992;
432 Wheeler et al., 2007) and may be associated with topographic features such as ridges
433 (Sula Ridge), escarpments (Pelagia Mounds) and channels (Hovland Mounds) (Wheeler
434 et al., 2007). Within the RD model reef habitat was clearly associated with bedrock
435 substrate, and ridge, escarpment, flank and pinnacle/mound features.

436

437 While fundamental questions remain concerning the physical factors that are
438 important in the development of reefs, recent research has highlighted the significance
439 of hydrodynamic conditions in reef formation. Reef habitat forms in areas of enhanced
440 turbidity, within a narrow density envelope, with high current velocities that prevent
441 local sedimentation but provide enhanced encounter-rates with food particles (Thiem
442 et al., 2006; Mienis et al., 2007; Dullo et al., 2008). These conditions must be stable
443 over long periods of time to allow reef development (Thiem et al., 2006). Inclusion of
444 hydrographic data in the model would undoubtedly improve the model fit and
445 predictive power, however fine scale oceanographic data are not widely available.
446 Geomorphology acts as a surrogate for fine scale current speed. The relationship
447 between reef habitat and geomorphological features such as ridges and escarpments
448 identified by the model most likely reflects both the substrate and hydrodynamic
449 requirements of reef habitat development.

450

451 **4.2 Importance of environmental parameters to predictive modelling of *L. pertusa***
452 **species and habitat distribution.**

453 Within both the SD and RD models, substrate, geomorphology and BPI were the most
454 important variables in terms of their importance to predicting species and habitat
455 distribution, followed by rugosity and slope for SD and depth and slope for RD. These
456 findings support those of Guinan et al. (2009a) who also found that at a slightly finer
457 but comparable spatial scale (30m multibeam grids) the most important variables in
458 predicting *L. pertusa* species distribution using GARP modelling, were rugosity and
459 slope. At finer resolution (0.5m multibeam grids) Dolan et al. (2008) found BPI,
460 structural complexity (fractal dimension) and orientation were important variables in
461 using ENFA modelling. At coarser resolution (550m grids) Guinan et al. (2009a) found
462 in addition to rugosity and slope, that aspect was weakly important. Neither Dolan et
463 al. (2008) nor Guinan et al. (2009) had produced interpreted layers for substrate and
464 geomorphology from multibeam bathymetry and backscatter and thus did not include
465 these variables in their models. Following these studies Guinan et al. (2009b)
466 concluded that coral abundance increases with increasing BPI, rugosity and slope.

467

468 Within the SD and RD models high positive BPI values were associated with high
469 probability of occurrence suggesting both species and habitat are associated with
470 raised features. High probability of species presence was also associated with high
471 negative BPI values, suggesting the species may be associated with depressions as well
472 as raised features. Probability of occurrence also increased with increasing rugosity

473 and slope to an asymptote (~1.16 and 30° respectively) suggesting values above this
474 may not increase the probability of presence.

475

476 **4.3 Implications for marine environmental management**

477 The difference in area identified by the models as suitable for the species compared to
478 the habitat has important implications for environmental management and the design
479 of marine protected area networks (MPAs). As reef distribution is a restricted subset of
480 species distribution, calculations of habitat extent based on the species distribution
481 (e.g. within a given countries EEZ or an area covered by a particular convention such as
482 OSPAR in the NE Atlantic), will be gross overestimates, and will thus mask the relative
483 rarity of the habitat. In addition, in the complex task of identifying suitable boundaries
484 for MPAs for the purpose of conserving reef habitat, boundaries drawn on the basis of
485 species distribution may fail to include the target habitat. It is therefore desirable,
486 where possible, to focus on the distribution of the habitat over the species at least at
487 fine scales. However, it would be unwise to consider *only* reef habitat distribution in
488 conservation planning, since connectivity between reef areas is likely to be maintained
489 by the wider species distribution. Isolated colonies on cobbles may well provide a
490 mechanism for gene-flow between larger reefs. This is particularly important as gene
491 flow occurring among subpopulations is moderate at best with high levels of
492 inbreeding and self-recruitment (Le Goff-Vitry et al., 2004). Research is needed into
493 issues of connectivity with respect to MPA planning.

494

495 The use of predictive species modelling in the deep-sea is a relatively new field.
496 Recently models constructed at global and regional scales used broad-scale
497 oceanographic data at cell sizes of 130km, 1 degree and 0.25° to predict the
498 distribution of *L. pertusa* species (Davies et al., 2008; Tittensor et al., 2009.). These
499 models identified the levels of nitrate silicate and phosphate, aragonite saturation,
500 dissolved oxygen, and percent oxygen saturation as important in predicting the
501 distribution of *L. pertusa*. The spatial resolution of the environmental data used in
502 these models (in many cases data derived from model predictions) are inadequate to
503 capture the fine-scale current regimes likely to determine the specific sites at which
504 reefs are present (Guinan et al., 2007). Therefore, while on global and regional scales a
505 focus on modelling (and mapping) the distribution of the species is useful and
506 appropriate for assisting in targeting and coordinating conservation efforts (Davies et
507 al., 2008; Tittensor et al., 2009), the discrepancy between the areas of predicted
508 presence of the species and the habitat in this study suggest that predictive modelling
509 of habitat distribution at fine scales is more useful in terms of identifying areas of reef
510 occurrence.

511

512 The importance of substrate, geomorphology, BPI, rugosity and slope to habitat
513 distribution reflect the hydrodynamic conditions required for reef formation. This is
514 important in terms of future mapping efforts. For *L. pertusa* reef, variables derived
515 from multibeam bathymetry and interpreted backscatter data collectively act as
516 suitable surrogates for those environmental factors, which are critical in determining

517 reef distribution, but for which we generally lack fine-scale data. This suggests that it
518 may be possible in future to undertake multibeam survey of appropriate resolution for
519 large areas of the deep-sea and from that produce reasonable maps of reef
520 distribution with limited ground truthing required. It also suggests that the final model
521 produced here could be used to predict the distribution of reef habitat in other areas.
522 However, the restricted depth and temperature range of the study area limits the final
523 model to use in areas of similar environmental conditions.

524

525 What constitutes an appropriate resolution (multibeam grid size) for a given accuracy
526 of predictive map requires further investigation if managers are to make informed
527 decisions to balance predictive accuracy with survey cost. In addition the inclusion of
528 interpreted substrate and geomorphology layers and their resulting importance in
529 both SD and RD models suggests that these variables are particularly useful in
530 providing good predictions. However, these interpretations take considerable time and
531 skill to produce. In practical terms there may be a trade off between the time (and
532 expense) taken to interpret such datasets and the gain in the accuracy of predicted
533 distributions. Further research is needed into assessing such tradeoffs in the
534 application of these methods.

535

536 **4.4 Use of Maxent in predictive modelling of biological community distribution**
537 **(biotope mapping).**

538 The use of predictive modelling in marine community mapping is in its infancy (Kelly et
539 al., 2001; Meleder et al., 2010). However, this technique has considerable benefits to
540 offer to conservation efforts in the deep-sea where areas are vast, biological data are
541 sparse and new survey is expensive. In shallow water areas remote sensing tools such
542 as airborne and satellite imagery and aerial photography may be used to map the
543 distribution of some habitats (Holmes et al., 2007). However, these tools rapidly reach
544 their limits for sub-tidal surveys because of the absorption of visible radiation by
545 water. At greater depths mapping is achieved using acoustic devices such as
546 multibeam and sidescan sonar which are then ground truthed using video or other
547 physical sampling methods (Brown et al., 2002; Huvenne et al., 2005; Brown and
548 Blondel, 2009; Buhl-Mortensen et al., 2009). Although methods of mapping benthic
549 assemblages vary, in general expert judgement is used to predict where assemblages
550 will occur based on where they have been observed. This effectively amounts to
551 predictive modelling using the mind. There is therefore a potential role for predictive
552 modelling in biological assemblage (or biotope as defined by Dahl (1908)) mapping
553 (Eastwood et al., 2006; Wilson et al., 2007). This study has demonstrated the potential
554 use of the freely downloadable software Maxent to model the distribution of *L.*
555 *pertusa* reef in benthic mapping efforts. This approach could be broadened and
556 applied to other listed biogenic habitats / biological communities such as coral
557 gardens, sponge aggregation etc, as well as any other defined benthic assemblages
558 (biotope).

559

560 **Acknowledgements**

561 The authors would like to acknowledge with thanks the scientists, officers and crew of
562 SV Kommandor Jack and MV Franklin, the staff at Geotek and Marin Mätteknik AB, the
563 wider project partners J. Davies, C. Marshall, S. Mowles, L. Robinson, C. Jacobs, N.
564 Golding, N. Coltman, and B. Narayanaswamy; also D. Bilton for helpful comments on
565 the manuscript, C. Embling for useful discussions on thresholding and modelling in
566 general, and two anonymous reviewers for their helpful comments. The collection of
567 data used within was funded by the Department for Business, Enterprise and
568 Regulatory Reform through Strategic Environmental Assessment 7 (formerly the
569 Department for Trade and Industry) and the Department for Environment, Food and
570 Rural Affairs through the their advisors the Joint Nature Conservation Committee and
571 the offshore Special Areas for Conservation programme. Data analysis was partly
572 funded by a mini grant awarded to K.L.H. from the Census of Seamounts, a joint
573 Research Councils of the UK fellowship awarded to K.L.H, and University of Plymouth,
574 and the ERASMUS student exchange programme. H.S. publishes with the permission
575 of the Executive Director of the British Geological Survey (NERC).

576

577 **References**

578 Anderson, R.P., Gómez-Laverde, M., Peterson, A.T., 2002. Geographical distributions
579 of spiny pocket mice in South America: insights from predictive models. *Global Ecol.*
580 *Biogeogr.* 11, 131– 141.

581

582 Auster, P.J., 2005. Are deep-water corals important habitats for fishes? in: Freiwald, A.,
583 Roberts, J.M. (Eds.), *Cold-Water Corals and Ecosystems*. Springer, Berlin, Heidelberg,
584 pp. 747–760.

585

586 Brown, C. J., Cooper, K. M., Meadows, W. J., Limpenny, D. S., Rees, H. L., 2002. Small
587 scale mapping of sea-bed assemblages in the eastern English Channel using sidescan
588 sonar and remote sampling techniques. *Estuar. Coast. Shelf Sci.* 54, 263–278.

589

590 Brown, C. J., Blondel, P., 2009. Developments in the application of multibeam sonar
591 backscatter. *Appl. Acoust.* 70, 1242–1247.

592

593 Bryan, T.L., Metaxas, A., 2007. Predicting suitable habitat for deep-water coral in the
594 families Paragorgiidae and Primnoidae on the Atlantic and Pacific continental margins
595 of North America. *Mar. Ecol. Prog. Ser.* 330, 113–126.

596

597 Buhl-Mortensen, P., Dolan, M., Buhl-Mortensen, L., 2009. Prediction of benthic
598 biotopes on a Norwegian offshore bank using a combination of multivariate analysis
599 and GIS classification. *ICES J. Mar. Sci.* 66, 2026–2032.

600

601 Cantor, S.B., Sun, C.C., Tortolero-Luna, G., Richards-Kortum, R., Follen, M., 1999. A
602 comparison of C/B ratios from studies using receiver operating characteristic curve
603 analysis. *Journal of Clinical Epidemiology* 52, 885–892.

604

605 Costello, M.J., McCrea, M., Freiwald, A., Lundalv, T., Jonsson, L., Brett, B.J., van
606 Weering, T.C.E., de Haas, H., Roberts, J.M., Allen, D., 2005. Role of cold-water *Lophelia*
607 *pertusa* coral reefs as fish habitat in the NE Atlantic, in: Freiwald, A., Roberts, J.M.
608 (Eds.), *Cold-Water Corals and Ecosystems*. Springer, Berlin, Heidelberg, pp. 771–805.

609

610 Dahl, F., 1908. Grundsätze und grundbegriffe der biocoenotischen forschung. *Zool.*
611 *Anz.* 33, 349-353.

612

613 Davies, A.J., Wisshak, M., Orr, J.C., Roberts, J.M., 2008. Predicting suitable habitat for
614 the cold-water coral *Lophelia pertusa* (Scleractinia). *Deep-Sea Res. Pt. I*, 55, 1048–
615 1062.

616

617 Dolan, M.F.J., Grehan, A.J., Guinan, J.C., Brown, C., 2008. Modelling the distribution of
618 cold-water corals in relation to bathymetric variables: adding spatial contact to deep-
619 sea video. *Deep-Sea Res. Pt. I*. 55, 1564–1579.

620

621 Dons, C., 1944. Norges korallrev. K. Norske Vidensk. Selsk. Forh. 16, 37–82.

622

623 Dullo, C.W., Flögel, S., Rüggeberg, A., 2008. Cold-water coral growth in relation to the
624 hydrography of the Celtic and Nordic European continental margin. Mar. Ecol. Prog.
625 Ser. 371, 165– 176.

626

627 Eastwood, P.D., Souissi, S., Rogers, S.I., Coggan, R.A., Brown, C.J., 2006. Mapping
628 seabed assemblages using comparative top-down and bottom-up classification
629 approaches. Can. J. Fish. Aquat. Sci. 63, 1536–1548.

630

631 Elith, J., Graham, C.H., Anderson, R.P., Dudík, M., Ferrier, S., Guisan, A., Hijmans, R.J.,
632 et al., 2006. Novel methods improve prediction of species' distributions from
633 occurrence data. Ecography 29, 129–151.

634

635 Embling, C.B., , Gillibrand, P.A., Gordona, J., Shrimpton, J., Stevick, P.T., Hammond P.S.,
636 2010. Using habitat models to identify suitable sites for marine protected areas for
637 harbour porpoises (*Phocoena phocoena*). Biol. Conserv. 143, 267-279.

638

639 Frederiksen, R., Jensen, A., Westerberg, H., 1992. The distribution of the scleractinian
640 coral *Lophelia pertusa* around the Faeroe Islands and the relation to internal tidal
641 mixing. *Sarsia* 77, 157–171.

642

643 Freeman, E., 2007. PresenceAbsence: An R Package for Presence-Absence Model
644 Evaluation. USDA Forest Service, Rocky Mountain Research Station, 507 25th street,
645 Ogden, UT, USA.

646

647 Freiwald, A., Fosså, J.H., Grehan, A., Koslow, T., Roberts, J.M., 2004. Coldwater Coral
648 Reefs. UNEP-WCMC, Cambridge, UK.

649

650 Guinan, J.C., Grehan, A.J., Wilson, M.F.J., Brown, C., 2009. Quantifying relationships
651 between video observations of cold-water coral and seafloor features in Rockall
652 Trough, west of Ireland. *Mar. Ecol. Prog. Ser.* 375, 125–138.

653

654 Guinan, J., Brown, C., Dolan, M.F.J., Grehan, A.J., 2009. Ecological niche modelling of
655 the distribution of cold-water coral habitat using underwater remote sensing data.
656 *Ecol. Info.* 4, 83-92.

657

658 Hitchen, K., 2004. The geology of the UK Hatton-Rockall margin. *Mar. Petrol. Geol.* 21,
659 993-1012.

660

661 Holmes, K.W., Van Niel, K.P., Kendrick, G.A., Radford, B., 2007. Probabilistic large-area
662 mapping of seagrass species distributions. *Aquat. Conserv.: Mar. Freshwat. Ecosyst.* 17,
663 385-407.

664

665 Hovland, M., 2005. Pockmark-associated coral reefs at the Kristin field off Mid-Norway,
666 in: Freiwald, A., Roberts, J.M. (Eds.), *Cold-Water Corals and Ecosystems*. Springer,
667 Berlin, Heidelberg, pp. 623–632

668

669 Howell, K.L., 2010. A benthic classification system to aid in the implementation of
670 marine protected area networks in the deep/high seas of the NE Atlantic. *Biol.*
671 *Conserv.* 143, 1041-1056.

672

673 Husebø, Å., Nøttestad, L., Fosså, J.H., Furevik, D.M., Jørgensen, S.B., 2002. Distribution
674 and abundance of fish in deep-sea coral habitats. *Hydrobiologia* 471, 91–99.

675

676 Huvenne, V.A.I., Beyer, A., de Haas, H., Dekindt, K., Henriët, J.P., Kozachenko, M., Olu-
677 Le Roy, K., Wheeler, A.J., 2005. The seabed appearance of different coral bank

678 provinces in the Porcupine Seabight, NE Atlantic, results from sidescan sonar and ROV
679 seabed mapping, in: Freiwald, A., Roberts, J.M. (Eds.), Cold-Water Corals and
680 Ecosystems. Springer, Berlin, Heidelberg, pp. 535-569.

681

682 Méléder, V., Populus, J., Guillaumont, B., Perrot, T., Mouquet, P., 2010. Predictive
683 modelling of seabed habitats: case study of subtidal kelp forests on the coast of
684 Brittany, France. *Mar. Biol.* 157, 1525-1541.

685

686 ICES., 2008. Report of the Working Group on the Biology and Assessment of Deep-Sea
687 Fisheries Resources (WGDEEP), ICES Headquarters, Copenhagen.

688

689 ICES., 2010. Report of the Working Group on Elasmobranch Fishes (WGEF), Horta,
690 Portugal.

691

692 Kelly, N.M., Fonseca, M., Whitfield, P., 2001. Predictive mapping for management and
693 conservation of seagrass beds in North Carolina. *Aquat. Conserv.: Mar. Freshwat.*
694 *Ecosyst.* 11, 437–451.

695

696 Le Goff-Vitry, M.C., Pybus, O.G., Rogers, A.D., 2004. Genetic structure of the deep-sea
697 coral *Lophelia pertusa* in the northeast Atlantic revealed by microsatellites and internal
698 transcribed spacer sequences. *Mol. Ecol.* 13, 537–549.

699

700 Liu, C., Berry, P.M., Dawson, T.P., Pearson, R.G., 2005. Selecting thresholds of
701 occurrence in the prediction of species distributions. *Ecography* 28, 385–393.

702

703 Mienis, F., de Stigter, H.C., White, M., Duineveld, G., de Haas, H., vanWeering, T.C.E.,
704 2007. Hydrodynamic controls on cold-water coral growth and carbonate-mound
705 development at the SW and SE Rockall Trough Margin, NE Atlantic Ocean, *Deep-Sea*
706 *Res. Pt. I* 54, 1655–1674.

707

708 Mortensen, P., Buhl-Mortensen, L., 2004a. Deep-water corals and their habitats in The
709 Gully, a submarine canyon off Atlantic Canada, in: Freiwald, A., Roberts, J.M. (Eds.),
710 *Cold-Water Corals and Ecosystems*. Springer, Berlin, Heidelberg, pp. 247–277.

711

712 Mortensen, P.B., Buhl-Mortensen, L., 2004b. Distribution of deep-water gorgonian
713 corals in relation to benthic features in the Northeast Channel (Atlantic Canada). *Mar.*
714 *Biol.* 144, 1223–1238.

715

716 Musgrove, F.W., Mitchener, B., 1996. Analysis of the pre-Tertiary rifting history of the
717 Rockall Trough. *Petrol. Geosci.* 2, 353-360.

718

719 Pearson, R.G., Raxworthy, C., Nakamura, M., Peterson, A.T., 2007. Predicting species'
720 distributions from small numbers of occurrence records: a test case using cryptic
721 geckos in Madagascar. *J. Biogeogr.* 34, 102–117.

722

723 Pearson, R.G., Dawson, T.P., Lin, C., 2004. Modelling species distributions in Britain: a
724 hierarchical integration of climate and land-cover data. *Ecography* 27, 285–298.

725

726 Phillips, S.J., Dudík, M., Schapire, R.E., 2004. A maximum entropy approach to species
727 distribution modelling, in: *Proceedings of the Twenty-First International Conference on*
728 *Machine Learning*, ACM Press, New York, pp. 83.

729

730 Phillips, S.J., Dudík, M., Schapire, R.E., 2006. Maximum entropy approach to species
731 geographic distributions. *Ecol Model.* 190, 231–259.

732

733 Phillips, S.J., Dudík, M., 2008. Modeling of species distributions with Maxent: new
734 extensions and a comprehensive evaluation. *Ecography* 31, 161–175.

735

736 R Development Core Team, 2010. R: A language and environment for statistical
737 computing. R Foundation for Statistical Computing, Vienna, Austria. ISBN 3-900051-07-
738 0, URL <http://www.R-project.org>.

739

740 Roberts, J., Wheeler, A.J., Freiwald, A., 2006. Reefs of the deep: the biology and
741 geology of cold-water coral ecosystems. *Science* 312, 543–547.

742

743 Thiem, Ø., Ravagnan, E., Fosså, J.H., Bersten, J., 2006. Food supply mechanisms for
744 coldwater corals along a continental shelf edge. *J. Mar. Syst.* 60, 207–219.

745

746 Tittensor, D.P., Baco, A.R., Brewin, P.E., Clark, M.R., Consalvey, M., Hall-Spencer, J.,
747 Rowden, A.A., Schlacher, T., Stocks, K., Rogers, A.D., 2009. Predicting global habitat
748 suitability for stony corals on seamounts. *J. Biogeogr.* 36, 1111–1128.

749

750 Weiss, A.D., 2001. Topographic Positions and Landforms Analysis. ESRI International
751 User Conference, San Diego, USA.

752

753 Wheeler, A. J., Beyer, A., Freiwald, A., de Haas, H., Huvenne, V.A.I., Kozachenko, M.,
754 Roy, K.O.L., Opderbecke, J., 2007. Morphology and environment of cold-water coral
755 carbonate mounds on the NW European margin, *Int. J. Earth Sci.*, 96, 37–56.

756

757 Wilson, J.B., 1979. 'Patch' development of the deep-water coral *Lophelia pertusa* (L.)
758 on Rockall Bank. *J. Mar. Biol. Assoc. UK.* 59, 165–177.

759

760 Wilson, M.F.J., O'Connell, B., Brown, C., Guinan, J.C., Grehan, A., 2007. Multiscale
761 terrain analysis of multibeam bathymetry data for habitat mapping on the continental
762 slope. *Mar. Geod.* 30, 3–35.

763

764 Zibrowius, H., 1980. Les Scleractinaires de la Mediterranee et de l'Atlantique nord-
765 oriental. *Mem. Inst. Oceanogr. (Monaco)* 11, p. 227.

766 Table 1: Sea-bed substrate and geomorphology classes identified on Hatton Bank and
 767 George Bligh Bank.

Code	Substrate	Geomorphology
1	Gravelly Sand	Scour
2	Gravel	Relatively Flat Lying Sea Bed
3	Bedrock	Pinnacle / Mound
4	Gravelly Muddy Sand	Escarpment
5	Sand	Iceberg Ploughmarks
6	Mud	Furrow
7	Sandy Gravel	Ridge Crest
8	Muddy Sand	Flank
9	null	Channel
10	Sandy Mud	Ridge
11	null	Depression

768

769 Table 2: Threshold dependent model performance metrics for SD and RD models for three different thresholding approaches.

SD models Threshold	Full model build data			Average training			Average test		
	PCC	sensitivity	specificity	PCC	sensitivity	specificity	PCC	sensitivity	specificity
Sensitivity-specificity equality	0.72	0.72	0.72	0.71 (0.08)	0.71 (0.08)	0.71 (0.08)	0.73 (0.12)	0.73 (0.12)	0.73 (0.12)
Sensitivity-specificity sum maximization	0.67	0.92	0.58	0.70 (0.05)	0.81 (0.17)	0.68 (0.07)	0.80 (0.10)	0.72 (0.16)	0.82 (0.10)
ROC plot-based approach	0.74	0.72	0.75	0.72 (0.03)	0.76 (0.13)	0.71 (0.03)	0.78 (0.10)	0.74 (0.14)	0.80 (0.10)
RD models									
Sensitivity-specificity equality	0.90	0.94	0.90	0.79 (0.05)	0.79 (0.05)	0.79 (0.05)	0.93 (0.08)	0.96 (0.10)	0.93 (0.08)
Sensitivity-specificity sum maximization	0.90	0.94	0.90	0.77 (0.14)	0.92 (0.11)	0.76 (0.14)	0.92 (0.11)	1.00 (0)	0.90 (0.13)
ROC plot-based approach	0.90	0.94	0.90	0.84 (0.11)	0.82 (0.07)	0.84 (0.11)	0.93 (0.08)	0.96 (0.10)	0.93 (0.08)

770
771

772 Table 3: Area Under the Curve (AUC) scores for SD and RD models for full models and
 773 all partitions of the occurrence data into training-test datasets.

	SD Model	Training AUC	Test AUC	RD Model	Training AUC	Test AUC
	Full model	0.964	0.808	Full model	0.998	0.940
	Cross validation models					
	1	0.839	0.695	1	0.924	0.792
	2	0.567	0.774	2	0.909	0.870
	3	0.856	0.744	3	0.946	0.912
	4	0.634	0.884	4	0.854	1.000
	5	0.797	0.721	5	0.876	1.000
	6	0.815	0.957	6	0.876	1.000
	7	0.822	0.854			
	8	0.821	0.802			
	9	0.828	0.627			
	10	0.830	0.973			
	Mean	0.781	0.803		0.897	0.929
774	Standard Deviation	0.098	0.113		0.035	0.087

774
775

776 **Figure Captions**

777 Figure 1: The study area with sample details shown. Depth contours taken from the
778 GEBCO digital atlas and are in 100m isobaths down to 1000m, thereafter in 500m
779 isobaths.

780

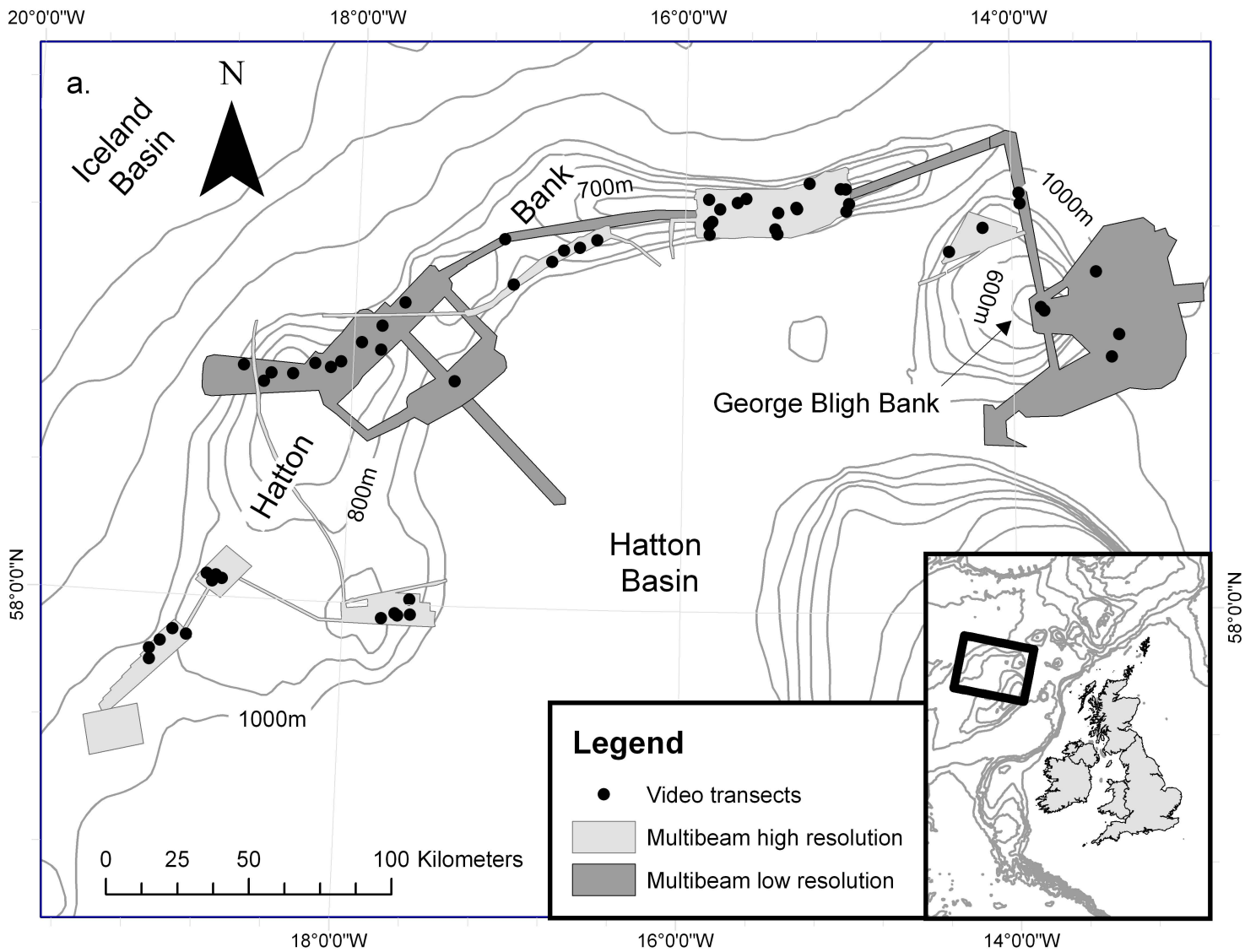
781 Figure 2: Jackknife of regularised training gain for a) *Lophelia pertusa* species and b)
782 *Lophelia pertusa* reef. “Without variable” – each variable is excluded in turn and a
783 model created with the remaining variables; “With only variable” – model constructed
784 using only one variable; “With all variables” – full model build.

785

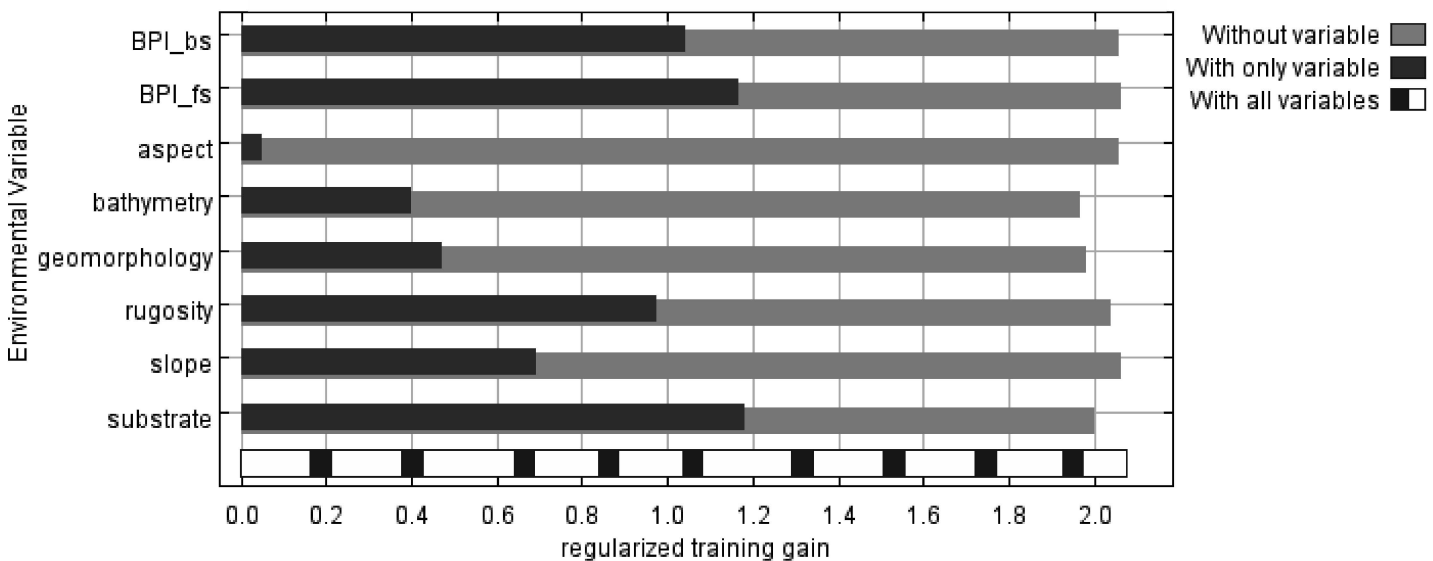
786 Figure 3: Response curves generated from a model built using only the corresponding
787 variable for a) *Lophelia pertusa* species and b) *Lophelia pertusa* reef. Y axis =
788 probability of presence, X axis label given above each plot, or for substrate codes 1-10
789 and geomorphology codes 1-11, see Table 1.

790

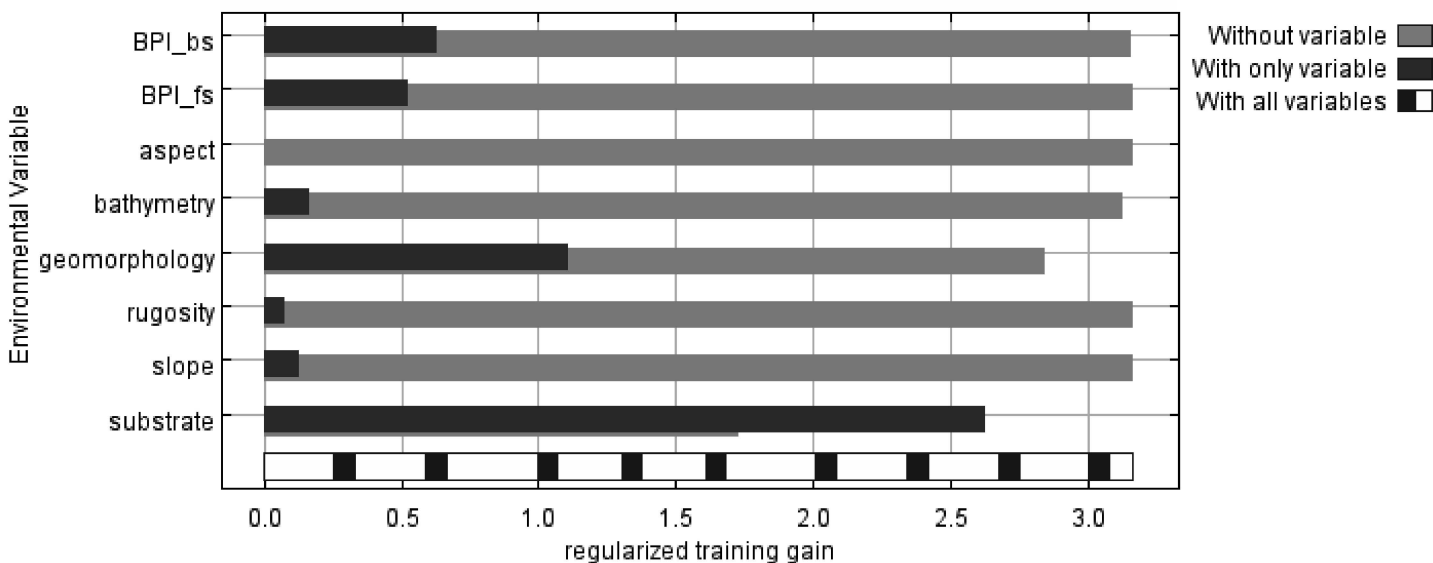
791 Figure 4: Modelled distribution of *Lophelia pertusa* species and *Lophelia pertusa* reef a)
792 on a subsection of Hatton Bank (inset) and b) on a small area identified in a. Maps c-e
793 show the individual environmental layers from the same area as b, and illustrate the
794 relationship between predicted presence areas and the 2 most important
795 environmental variables in each model.

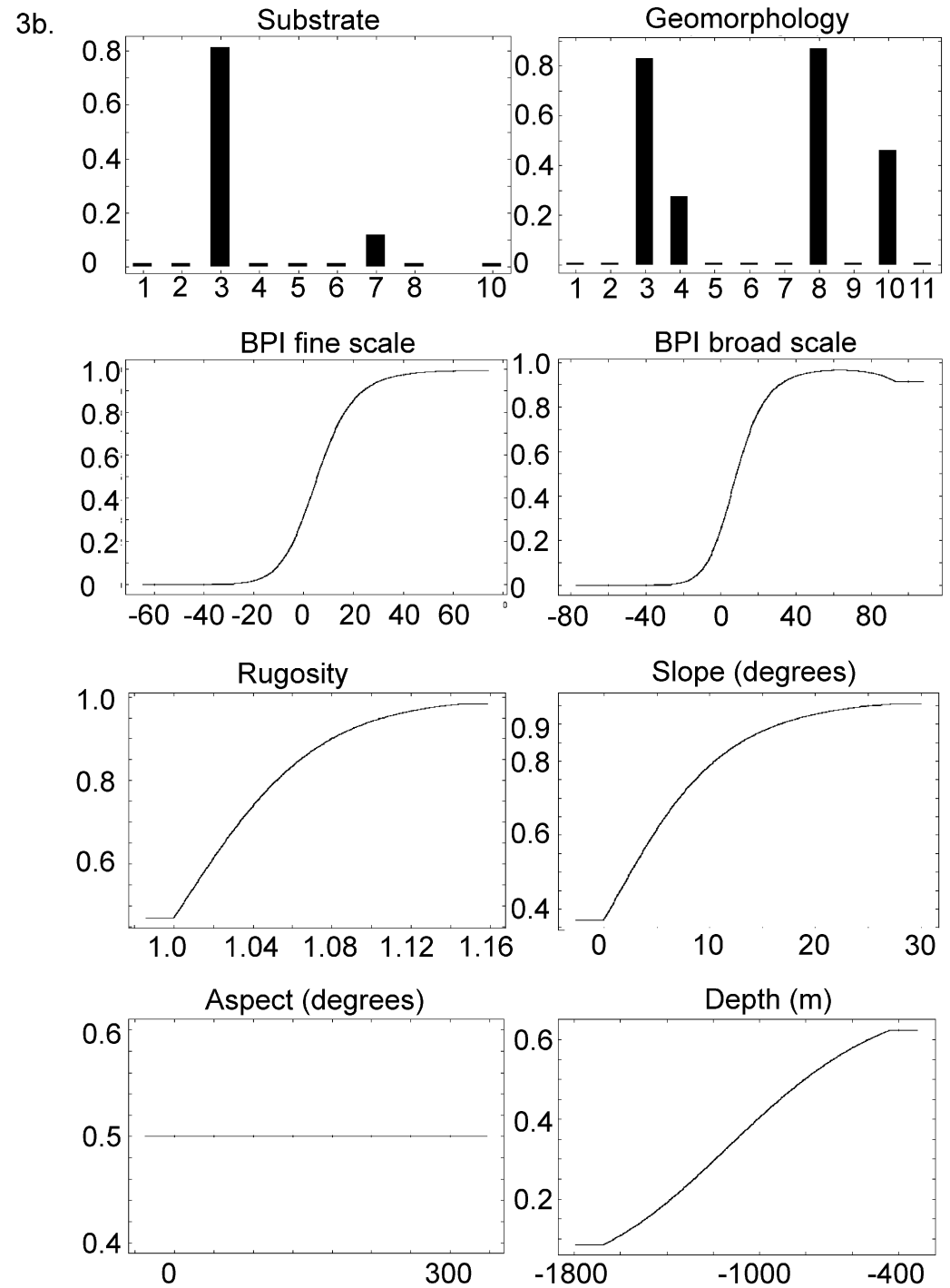
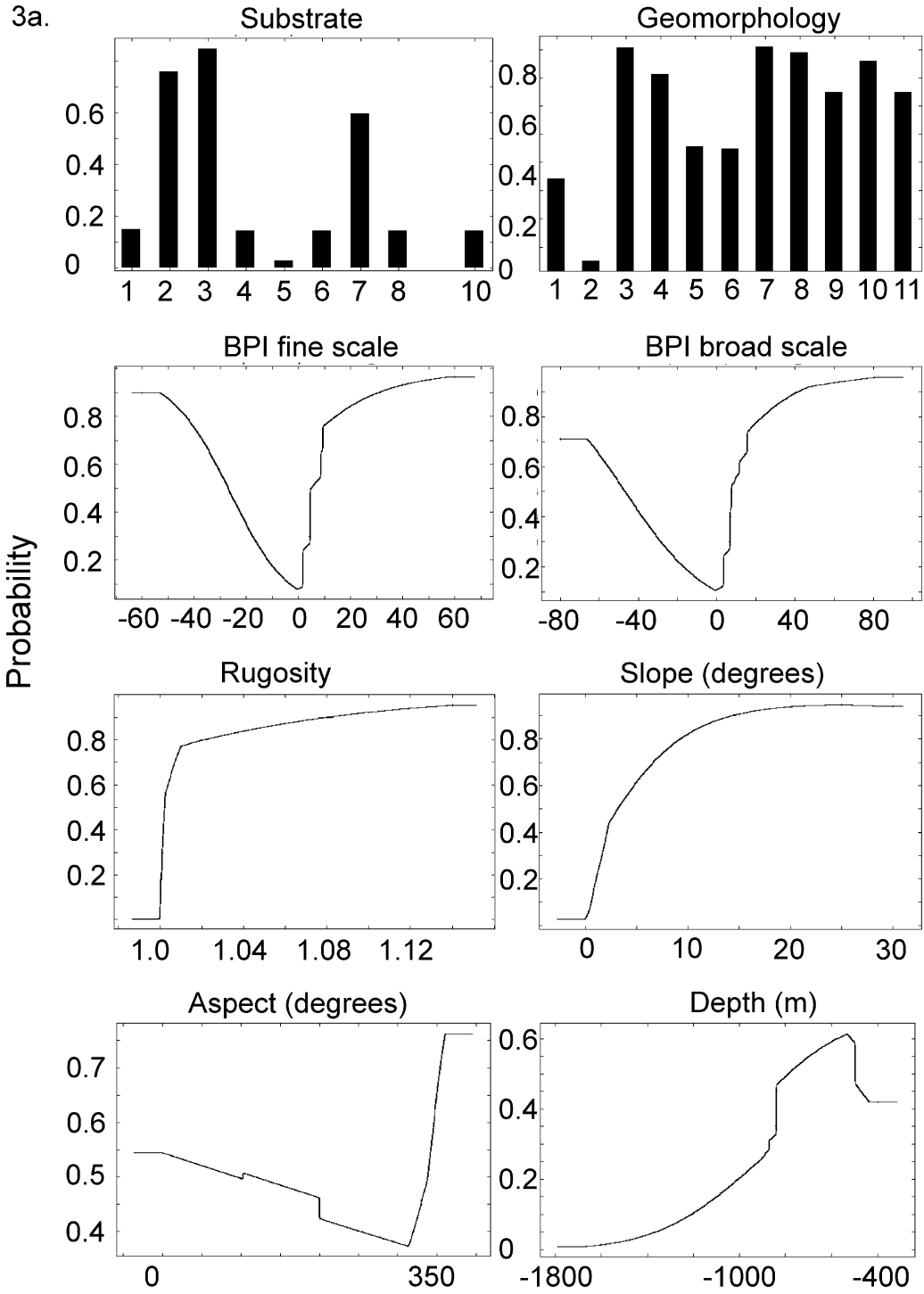


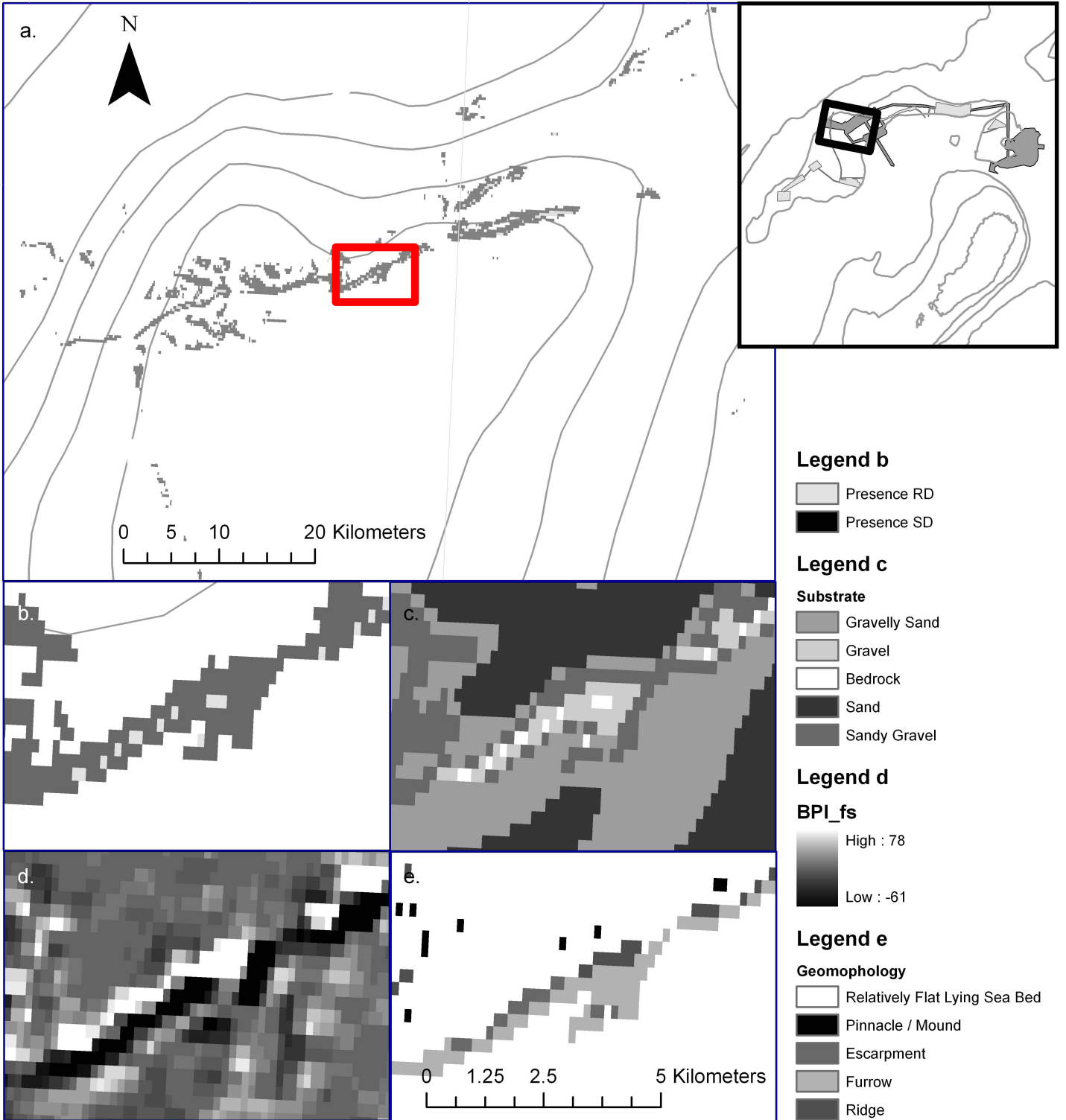
a.



b.







SD Model	Training AUC	Test AUC	RD Model	Training AUC	Test AUC
Full model	0.964	0.808	Full model	0.998	0.940
Cross validation models					
1	0.839	0.695	1	0.924	0.792
2	0.567	0.774	2	0.909	0.870
3	0.856	0.744	3	0.946	0.912
4	0.634	0.884	4	0.854	1.000
5	0.797	0.721	5	0.876	1.000
6	0.815	0.957	6	0.876	1.000
7	0.822	0.854			
8	0.821	0.802			
9	0.828	0.627			
10	0.830	0.973			
Mean	0.781	0.803		0.897	0.929
Standard Deviation	0.098	0.113		0.035	0.087